Manufacturing and durability of alkali activated mortars containing different types of glass waste as aggregates valorisation

Manufacturing and durability of alkali activated mortars containing different types of glass waste as aggregates valorisation

Andrea Saccani[1], Stefania Manzi[1*], Isabella Lancellotti[2], Luisa Barbieri[2]

[1]Department of Civil, Chemical, Environmental and Materials Engineering, University of Bologna, Via Terracini 28, 40131 Bologna, Italy

[2]Department of Engineering "Enzo Ferrari", University of Modena and Reggio Emilia, Via Vivarelli 10, 41125 Modena, Italy

Corresponding author*: stefania.manzi4@unibo.it, +39 051 2090329

Abstract

Mortars containing glass waste as a partial substitution for natural sand have been formulated. Alkali activated fly ashes have been used as a binder. The selected cullets are those deriving either from the discarded lamps collection or the fraction of the selective urban glass collection (about 10 wt% on the whole amount) that, because of its highly heterogeneous composition, cannot be used in the production of new glass items. Mechanical properties of the obtained mortars have been investigated as well as their durability. In details, the reactivity towards alkali silica reactions and sulphates

diffusion, as well as the stability to freeze-thaw cycles have been compared to the ones of unmodified mortars. Both types of waste do not lead to a decrease in the durability of the obtained materials. The inertness of these cullets towards alkali silica reaction is quite remarkable since both wastes are highly reactive in Portland cement matrix. This introduces a possible reuse in the formulation of low-impact renders for these fractions that presently have no alternatives to landfilling.

Keywords

Glass waste; separated urban collection; lead containing glass; aggregates for building materials; alkali activated fly ashes; ASR; durability.

1. Introduction

Glass recycling is not a closed-loop system. Due to the scanty quality of the urban collection, to the erratic conferring of many domestic items and to the limits of the separation that can be performed in sorting plants, around 10% of the overall collected amount of glass is disposed in landfills [1]. According to the European Waste Catalogue (EWC) [2], the code (19 12 05) is assigned to this fraction. The composition of this material is rather heterogeneous. Crystal items (containing at least 25 wt.% of lead oxide), ceramics (including porcelain), Pyrex (borosilicate glass), light bulbs, neon tubes, mirrors, television and computer monitors (like cathode ray tubes (CRTs) and liquid crystal displays (LCDs)) and other inert materials, are wrongly considered to be

assimilated to packaging glass and consequently delivered in the bottle bank. A further example of unrecycled glass is that deriving from the separated collection of discarded lamp cullets. In this case, the presence of a small amount of lead oxide (< 1% wt) again classify this waste as special ones (European catalogue Code 19 12 05).

A possible way to prevent damping is the use of cullet as a substitute of natural sand in mortars [3-17]. Soda-lime glass recycling in building materials creates many benefits to the environment and justifies the presence of many researches present in literature. When using a Portland cement matrix, the main problem arising from the presence of glass cullets is the occurrence of alkali-silica reactions (ASR). Soda-lime glass [18-24], the first composition to be studied, being the more diffused one since it derives from packaging items, shows a limited reactivity towards alkalis. This partial reactivity depends on the presence of chromophore ions in the amorphous network, indeed to the glass colour. For example, flint glass is less reactive than brown and green ones [23]. Glass having more complex chemical composition and different origin, especially those containing heavy metals like lead, barium and strontium, have proved to be extremely deleterious forming highly expanding reaction products [25-29]. Although the problem can be prevented by the use of pozzolanic binders as a partial Portland substitution [30-33] or by some surface treatments that can change the glass chemical composition [34-36], other solutions can prove to be more convenient. In the last years, great attention has been attracted by alkali activated materials [37-40]. These binders have lower

carbon dioxide footprint than Portland cement and can give rise to large environmental benefits when deriving at least partially from industrial wastes. Moreover, preliminary researches [41-43] have also underlined how aggregates expanding in Portland cement mortars can became innocuous with alkali activated binders. In the present research, the durability of mortars formulated with alkali activated fly ashes and the two different types of waste glass previously described, i.e. the discarded fraction of the separate urban collection and separately collected fluorescent lamp are investigated. Both types of cullet had proved to be extremely reactive towards ASR in Portland matrix composites [44]. It seemed thus interesting to study their behaviour in a different matrix, to determine whether this could inhibit alkali silica reactions. Moreover, other durability aspects, such as the resistance to freeze-thaw cycles and the possible deleterious reactions triggered by sulphates diffusion on geopolymer binders play an important role in the future development of these materials. Many researches have been recently carried out on these subjects [45-49]. Consequently, in this research the effect of these recycled cullets on the durability of mortars has been studied in presence of these environmental stresses. An unmodified standard Portland mortar has been tested in the same conditions for comparison sake.

2. Experimental

2.1 Materials

2.1.1 Glass wastes

Crashed residuals of separate glass waste collection (that will be defined as Residuals of Urban Collection, RUB in the subsequent text) were kindly supplied by CoReVe (Consortium for Glass Recycling, Italy). This is a rather heterogeneous material. Fragments of ceramics, pebbles, mirrors splinters and light bulbs are mixed with glass cullet of different colour. Figure 1 shows the morphology of the wastes. The material is used without any sorting, that is to say, with all its contaminants. Consequently, the average chemical composition of the material was obtained by insulating a representative sample of 1 kg, collected by quartering. The sample was remelted at 1450°C in electric oven and quenched at room temperature. A homogeneous glassy specimen was obtained. Fragments herein obtained were analysed by energy-dispersive spectrometer EDS (microanalyzer Inca-350, Oxford Instruments) in different areas of its surfaces. The average chemical composition is reported in Table 1.

Lamp glass (LMP in the subsequent text) is deriving from a separated collection whose composition, derived with the same procedure, is also reported in Table 1.

Table 1. Oxide content of the investigated materials.

Material	SiO_2	Al_2O_3	Na_2O	K_2O	CaO	MgO	PbO	BaO	Fe_2O_3	SO_3	LOI
RUB	66.25	1.88	9.42	5.98	5.60	1.65	6.91	2.21	0.00	0.00	0.00
LMP	68.47	2.26	17.65	1.61	5.13	2.98	0.79	0.95	0.00	0.00	0.00
Fly ash	49.37	29.23	0.05	0.60	6.63	1.05	0.00	0.00	2.71	0.33	3.28

Figures 1(a) and 1(b) show the morphology of the crashed material obtained by optical microscopy. The as-received RUB and LMP wastes were dry-grounded in a laboratory ball mill to get particles between 0.075 and 2.00 mm with size distribution close to that of normalized sand that is reported in Figure 2.

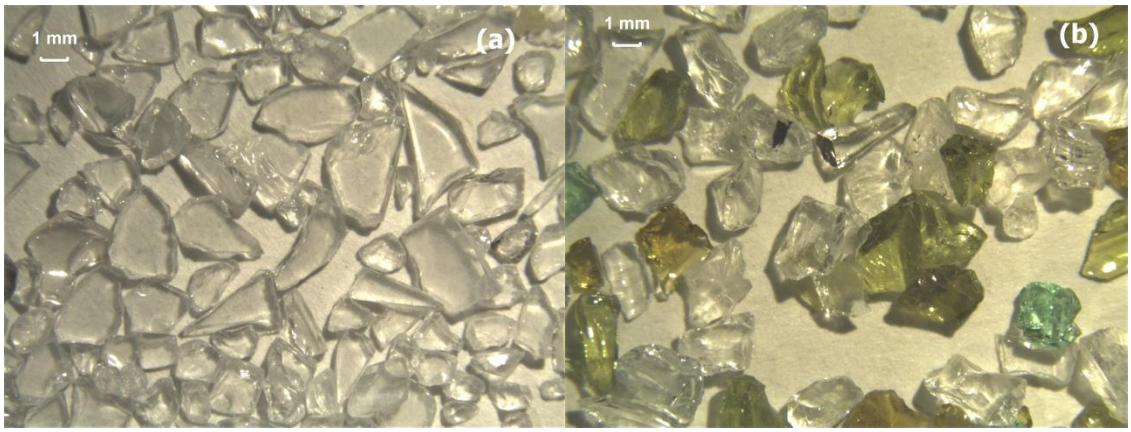

Fig. 1. Morphology of LMP (a) and RUB (b) cullets.

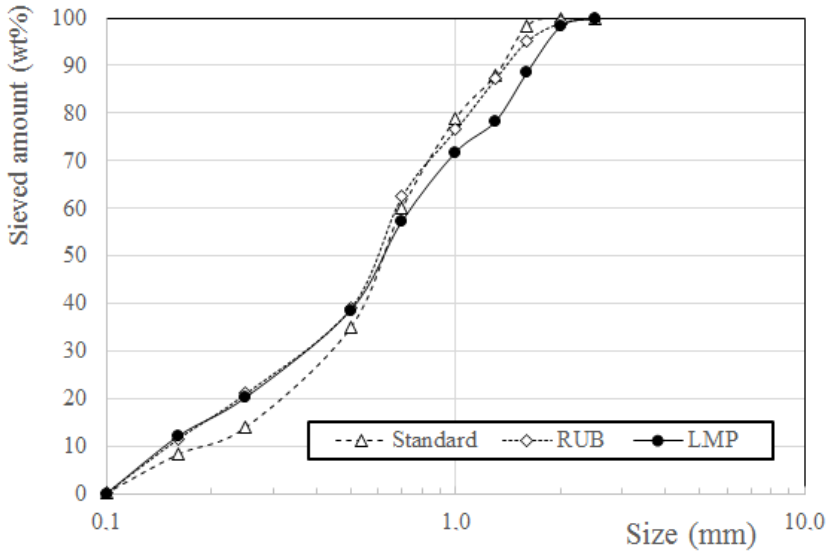

Fig. 2. Size distribution of natural sand and glass cullets.

2.1.2 Natural aggregate

Normalised silica sand conforming to the EN 196-1 Standard [50] was used. The size distribution is reported in Figure 2.

2.1.3 Binders

Fly ashes (Type F), whose chemical composition is reported in Table 1, deriving from the plant of Torrevaldaliga (Roma, Italy) were used. They have an average dimension (D_{50}) of 22 μm.

Portland cement Type II / AL 42.5 was used (Italcementi, Bergamo, Italy).

2.1.4 Activators

The sodium silicate solution used was a viscous liquid produced for the cement industry (Ingessil, Verona, Italy) with a water content of 56 wt%, the SiO_2/Na_2O oxide composition ratio of 2.07 and a density of 1.53 g/cm^3.

An 8 M water solution of sodium hydroxide (reagent grade form Carlo Erba, Milano, Italy) was used.

2.2 Mortars preparation

Mortars containing glass wastes (M-RUB and M-LMP in the subsequent text) were mixed by substituting 20 wt.% of natural siliceous sand. The binder/aggregate (b/a) ratio was 1.00/3.00. For samples to be submitted to ASR expansion test, a b/a ratio of 1.00/2.25 was used instead. Table 2 reports the mix design of all the investigated mortars and their relevant denomination, which will be used afterwards in the text. Mix

design, that is the ratio between fly ashes, activators and water was performed according to a previous research [39] in order to obtain Na_2O/SiO_2 and Na_2O/Al_2O_3 ratios of 0.12 and 0.42 respectively. This composition allowed to obtain good mechanical properties. As a reference, M-REF mortar was prepared with 100 wt.% of natural sand. Mixing was performed by first adding sodium hydroxide to the fly ashes and subsequently pouring the silicate in the vessel. After 3 minutes of stirring, glass waste was added to the paste, followed by the natural sand. The whole procedure lasts for 10 mins. In order to provide a benchmark, a mortar with standard composition (water/binder w/b 0.5 and b/a 1.00/3.00) was formulated using a traditional Portland 42.5 Type cement [50] (M-PRT in the subsequent text). Mixing procedures for this mortar followed the instruction of EN 196-1 [50].

Table 2. Composition and labelling of all investigated samples.

Mortar sample	Natural sand (g)	Glass waste (g)	Sodium silicate solution (g)	NaOH 8M solution (g)	H_2O (g)	Fly ash (g)	Portland cement (g)
M-REF	1350	0	188	38	35	500	-
M-RUB	1080	270	188	38	35	500	-
M-LMP	1080	270	188	38	35	500	-
M-PRT	1350	0	0	0	225	-	450

After the mixing process, mortars were cast in a truncated conical mould having a circular base (100 mm of diameter at the bottom, 70 mm of diameter at the top and 60 mm height, according to EN 1015-3 [51]). The mould was subsequently removed and the mortar shaken by means of a jolting device. The final dimension (i.e. the diameter) of the collapsed mortar was measured in two perpendicular directions and the workability (W) was thus calculated according to Eq. (1)

$$W = 100 \times (d_m - d°) / d° \quad (1)$$

where d_m is the average diameter of the two readings and d° is the lower diameter of the truncated conical ring, i.e. 100 mm.

The mixed mortars were cast in steel moulds to obtain 40 x 40 x 160 mm samples. In order to partially eliminate entrapped air and ensure an efficient filling of the moulds mortars were subjected to a defined number of jolts applied by means of a standardized jolting apparatus. Mortar samples were subsequently demoulded after a 24 h storage at 98 % R.H. and kept at 20 ± 1 °C in sealed polyethylene bags.

2.3 Instruments and methods

2.3.1 Density and porosity

Mortars density has been determined according to the EN 772-13 Standard [52] at 28 days of curing.

Porosity was calculated by determining the amount of absorbed cold water at atmospheric pressure following the EN 772-21 Standard [53] at 28 days of curing.

2.3.2 Expansion test

Alkali silica reactivity was evaluated according to the procedure described by ASTM C1260 [54], i.e. curing the specimens in moisture saturated conditions for 28 days, one day water curing at 80°C and subsequent storage at 80 °C in a 1 M solution of sodium hydroxide. The test was performed on three different samples for each of the investigated compositions.

2.3.3 Mechanical test

Mechanical tests (compression) on all samples were performed at room temperature and R.H. 50 ± 10 % by means of 100 kN Volpert Amsler equipment with a 50 mm/min displacement rate. The test was repeated on six samples at 28 days of curing.

2.3.4 Sulphates penetration

Samples with the standard dimension (40 x 40 x 160 mm) after 28 days of curing were soaked in a 1M Na_2SO_4 solution. At scheduled times, the dynamic elastic modulus was determined by means of a MATEST mod C369 (Treviolo, Italy). Equation (2) was applied to calculate the modulus value:

$$E = \rho \cdot V^2 \quad (2)$$

where:

V is the measured pulse velocity (m/s) and ρ is the density expressed in kg/m^3.

2.3.5 Freeze-thaw cycles

Samples having the same geometry and curing as before were submitted to freeze-thaw cycles according to ASTM C666 [55] that is (a) keeping samples at –10 ° C (b) subsequent thawing at 4 °C. At scheduled times the dynamic elastic modulus was determined according to the previous procedure.

2.3.6 Microstructure

Analyses were performed by means of a Quanta (FEI) scanning electron microscope equipped with an EDS X-ray detector. The fractured surfaces to be examined were coated by graphite to ensure electrical conductivity. Accelerating voltage of 20 kV was applied during all measurements.

3. Results and discussion

Table 3 reports the workability (expressed according to equation 1) of all the investigated mortars. The addition of both LMP and RUB increases the workability of mortars as compared to the one containing only natural sand. This effect has been already observed in literature for similar cullet additions [21, 43, 56] and has been ascribed to the smoother and less porous surface of the particles that tends to absorb less water than natural sand, thus changing the viscosity of the matrix. The density and the open porosity of the samples are also reported in Table 3. Both parameters remain almost constant as the natural sand is substituted for the wastes. The slight reduction in

density of M-RUB and M-LMP samples can be explained by the lower density of the cullets compared with the one of natural sand. The benchmark mortar (M-PRT) has a lower workability and a higher porosity.

Table 3. Physical properties of the investigated mortars.

Sample	M-REF	M-LMP	M-RUB	M-PRT
Workability (%)	59.1 ± 0.6	69.6 ± 0.9	69.0 ± 0.4	41.3 ± 0.8
Density (g/cm^3)	2.11	2.07	2.03	2.11
Porosity (vol %)	10.76	10.69	10.86	19.50

Figure 3 reports the expansion (1M NaOH solution, 80°C) of mortar samples formulated with and without the wastes. The acceptable limit, defined by the ASTM C1260 Standard [54], as the one ensuring an innocuous behaviour of the aggregates is of 0.1%. Although this limit has been formulated for traditional Portland cement composites, the same value will be used for alkali activated composites. Indeed, all the investigated mortars fall below this limit after the prescribed curing time of 14 days.

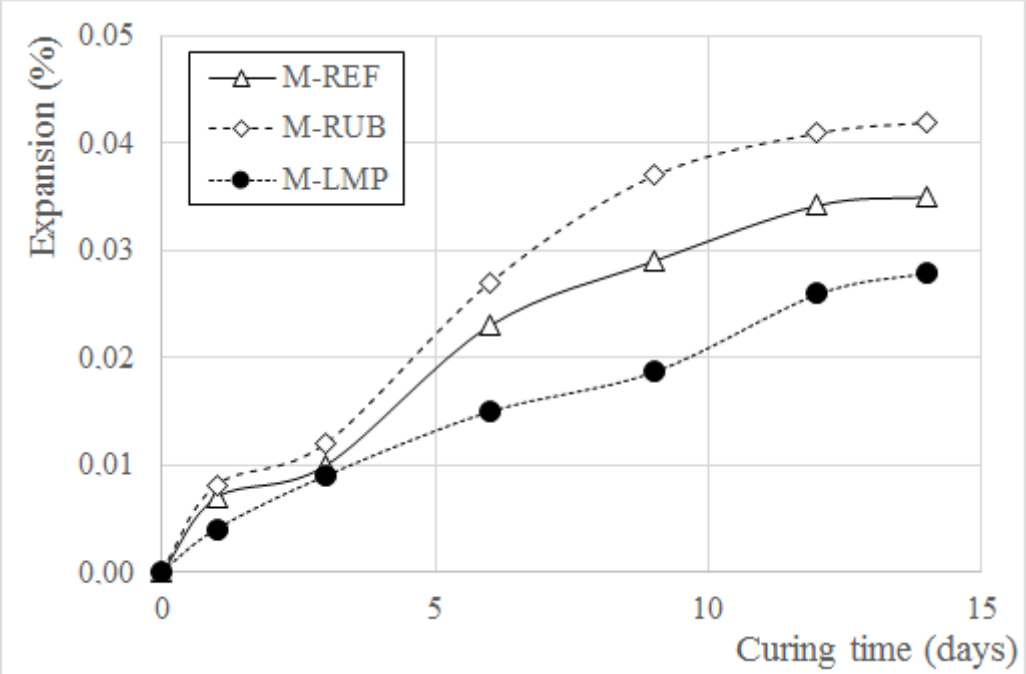

Fig. 3. Expansion at 80°C.

Figure 4 shows an example of the morphology of LMP cullets on the fractured surface of M-LMP mortar treated at 80°C after 14 days of curing. The transition zone between the aggregate surface (white arrow) and the matrix shows no expanding products and appears as unreacted. The morphology of RUB cullets in the same conditions is reported in Figure 5 for M-RUB mortar, disclosing a similar aspect.

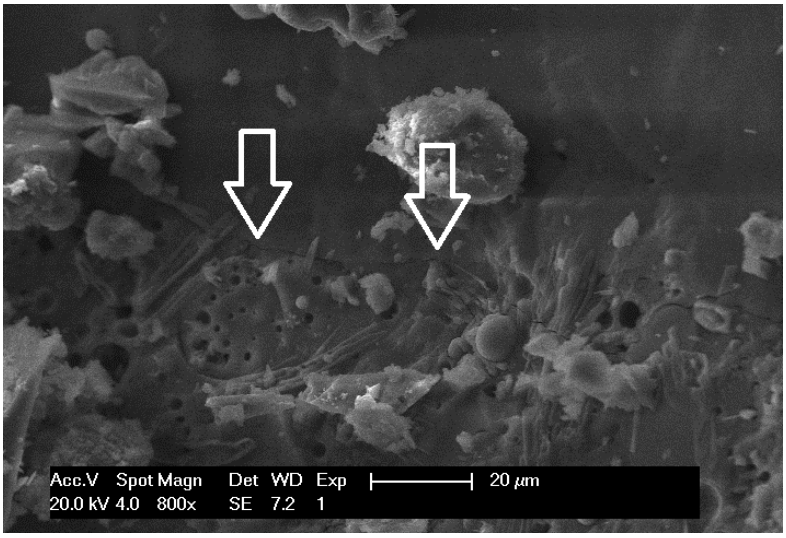

Fig. 4. Sharp unreacted contour (arrows) of one LMP cullet in contact with the alkali activated matrix (fracture surface of M-LMP cured at 80°C in NaOH solution).

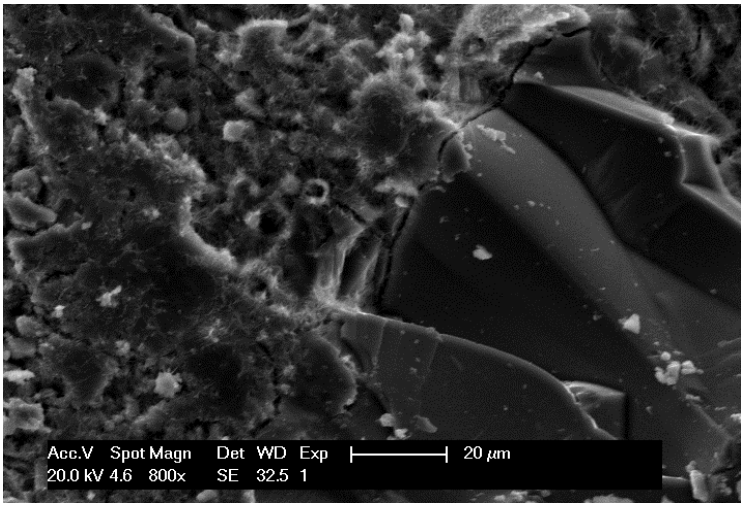

Fig. 5. Sharp unreacted RUB cullet cured at 80 °C in NaOH solution from M-RUB mortar.

Figure 6 reports the expansion of mortars cured at 38°C. As recorded before, all samples behave similarly and a quite limited expansion is detected even at the longest curing time. SEM observations (Figures 7 and 8) disclose the non-reactive behaviour of both LMP and RUB cullets respectively, showing unreacted surfaces. These results confirm that alkali activated fly ash systems are quite efficient in preventing ASR as found elsewhere [41, 42]. On the contrary, Portland cement mortars had previously shown strong expansion of both type of cullets [44].

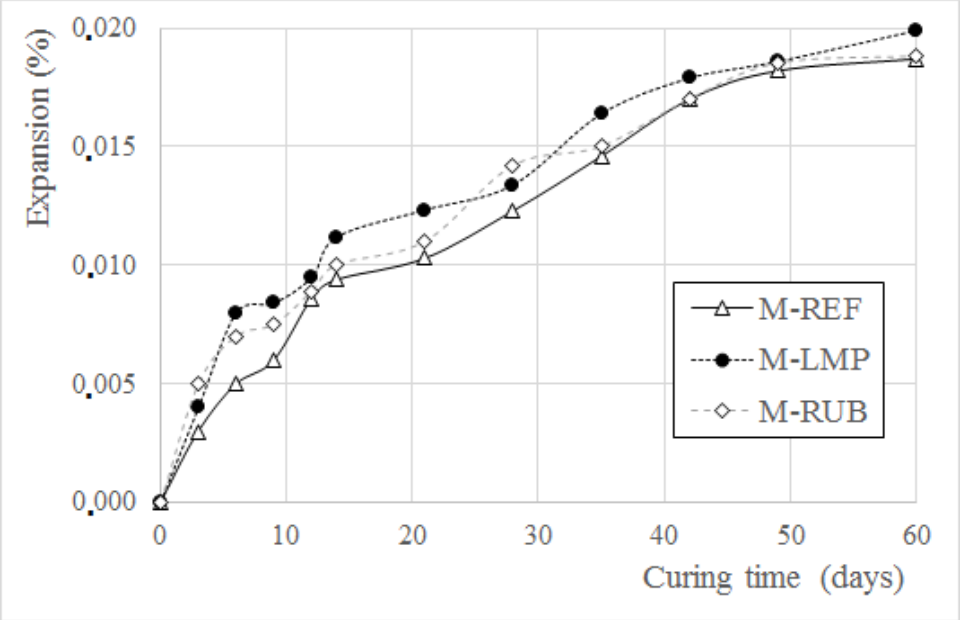

Fig. 6. Expansion vs curing time at 38°C.

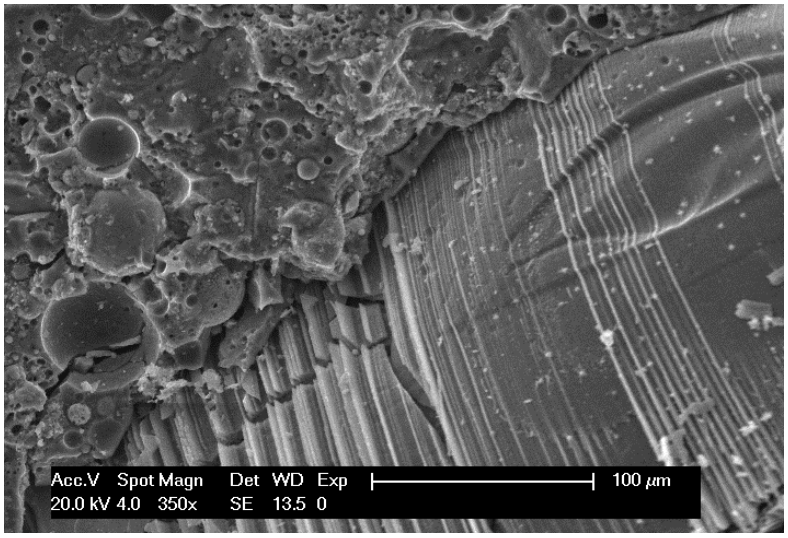

Fig.7. Unreacted LMP cullet at 60 days of curing (38 °C) for M-LMP mortar.

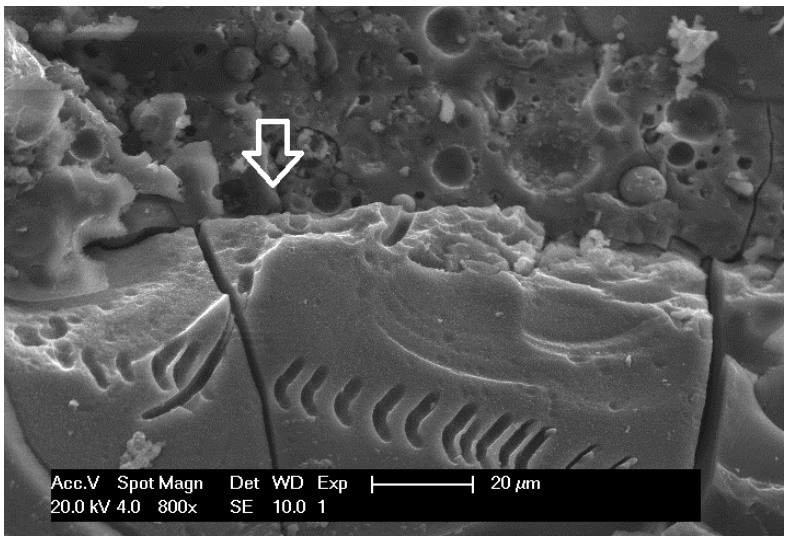

Fig. 8. Unreacted RUB cullet at 60 days of curing (38°C) for M-RUB mortar.

The average compressive strength of mortars after the different curing conditions (28 days at room temperature, end of the accelerated test for alkali reactivity at 80 °C and

38 °C) is reported in Figure 9. It should be noted that the alkali activated binder provides, in all cases, values comparable to the Portland mortar after 28 days of curing at room temperature. M-RUB and M-REF samples show comparable values of strength, while M-LMP samples have slightly higher values (about 10%). Mechanical results obtained after the accelerated ASR tests both at 38 and 80 °C show increased values than those obtained after 28 day of curing. This confirms that no expanding reactions take place during the tests since the mechanical properties are not compromised. Moreover, the higher temperatures and, in the case of the 38 °C the longer curing times, favour the development of the alkali activated network. The higher strength values found in M-LMP samples, especially cured for 28 days at 20°C and for 14 days at 80 °C in a 1M NaOH, is probably deriving from the sharp flat morphology of the cullets that provides higher mechanical interaction with the matrix than that of the roundish sand particles. A further contribution could arise from the increased alkalinity present at the interphase between matrix and cullet. The partial glass dissolution, taking place in the alkaline environment, as recently found in other researches [57], can influence the chemistry of the reactions involved in the matrix development. The extent of glass dissolution in this system should however be limited, since no clear evidence of dissolution could be detected from SEM observations.

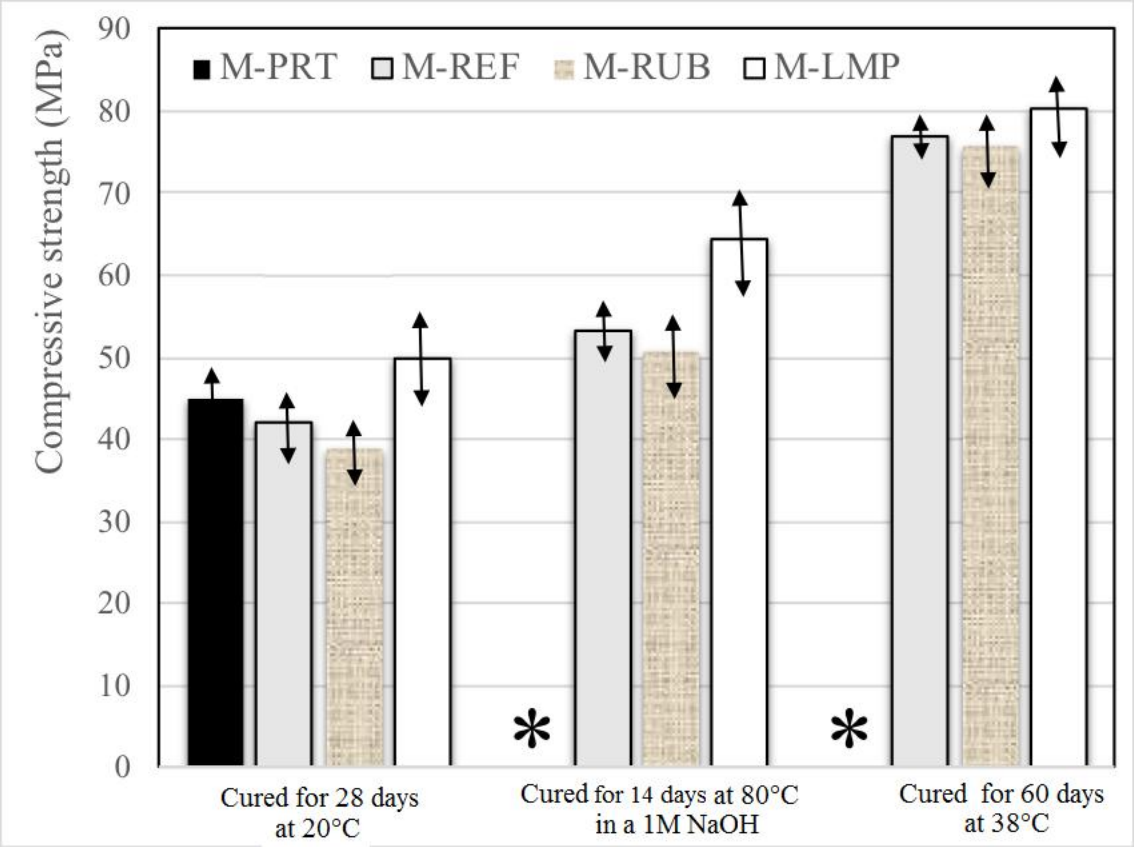

Fig. 9. Mechanical properties of samples in different curing conditions.

(*) Portland samples not reported since showing expanding behaviour

As to what concerns the effect of sulphates diffusion, in Figure 10 the value of the elastic modulus determined though the pulse velocity (Equation 2) is reported.

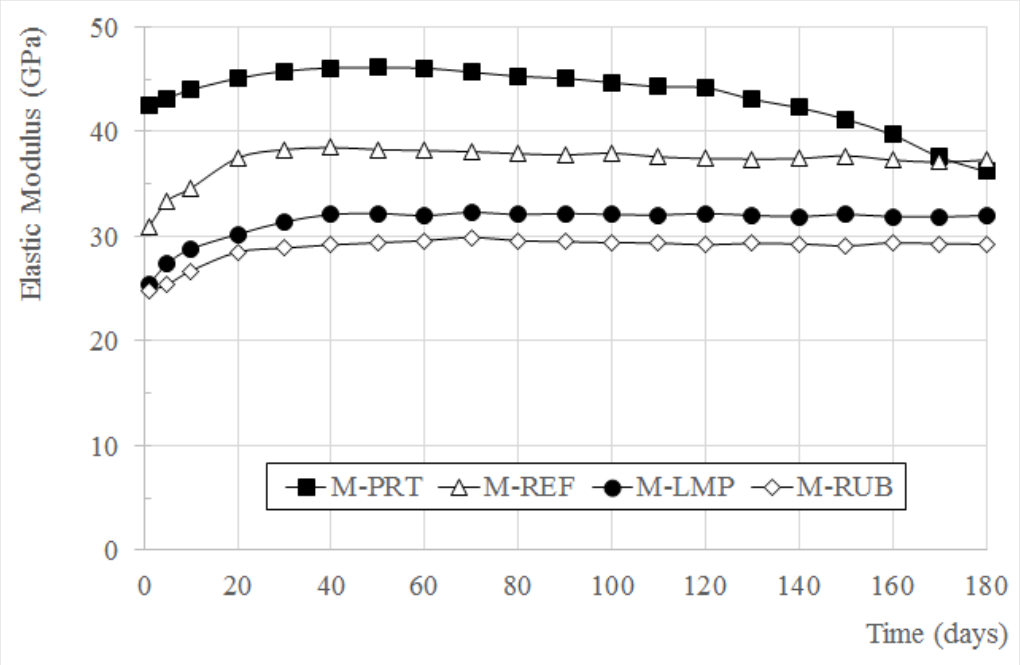

Fig. 10. Plot of the dynamic elastic modulus vs time of mortars in sulphates solution.

All samples formulated with the alkali activated matrix show an increase in the elastic modulus during the first stages, reaching an asymptotic value at the longest curing times. This trend is not depending on the aggregate type and it is thus depending only on the matrix strength. Mortar formulated with Portland cement (M-PRT) shows a clear decrease after about 120 days of exposure. In order to confirm the induced damage in these mortars, SEM observations were carried out collecting samples at the longest curing times (180 days). Figure 11(a) shows the ettringite crystals on M-PRT mortars and 11(b) the microstructure of M-RUB sample, similar to M-LMP and M-REF, for sake of comparison.

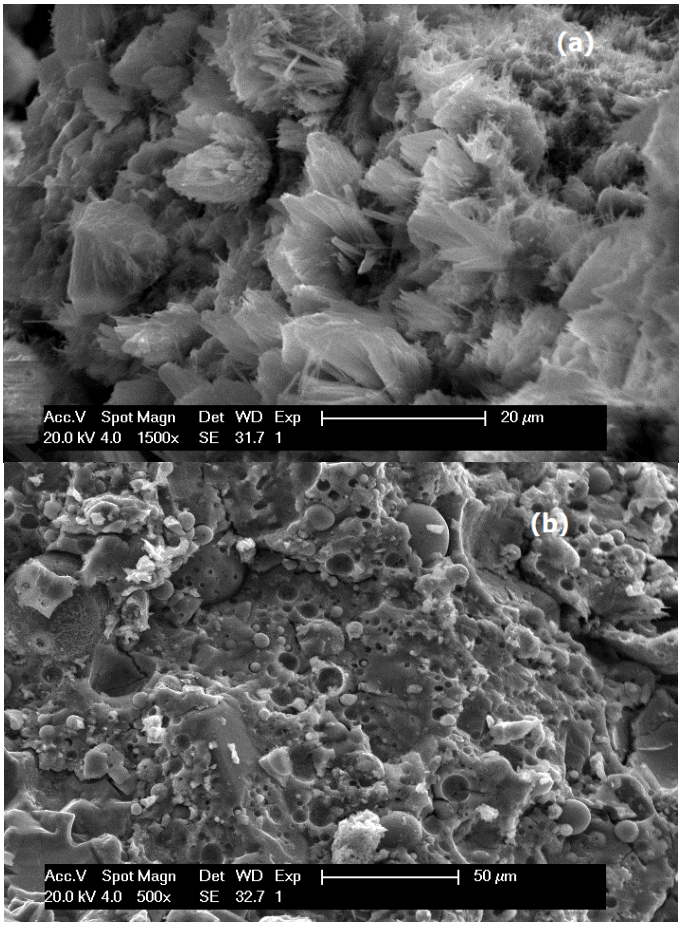

Fig. 11. (a) ettringite samples in M-PRT sample (b) alkali activated matrix of M-RUB sample.

Figure 12 reports the trend of the elastic modulus of all the investigated mortars submitted to freeze-thaw cycles. The values of the modulus show a slight decrease as the number of cycles increases in all the samples. The extent of this progressive decrease is comparable in all formulations ranging from a 9.4 % in M-REF to a 6.1 % in

M-RUB sample of the initial value (Portland mortar shows an 8% reduction, M-LMP an 8.6%). Alkali activated materials prove thus to perform similarly to traditional standard Portland composites. Moreover, the use of both wastes does not compromise the durability.

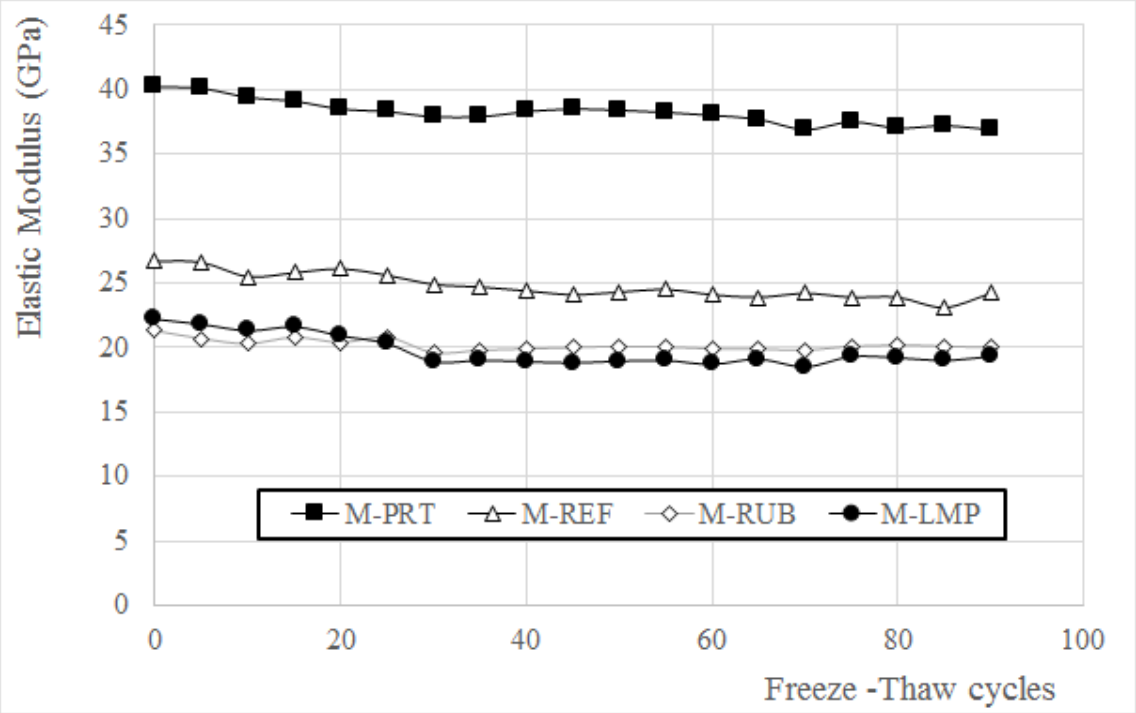

Fig. 12. Elastic modulus vs freeze-thaw cycles.

Up to now, alkali activated materials are not usually applied in structural application mainly due to the absence of *ad-hoc* standards. Their use can thus be limited to low demanding application such as renders, conduits, sewer pipes or drainage channels. In

this context, the low-impact environmental characteristics of the investigated materials as well as their increased sulphates durability compared to traditional Portland cement mortars, offer an important advantage. It is thus possible to prevent cullet damping and reduce natural sand extraction, both factors reducing also the overall final cost of the composite.

4. Conclusions

Alkali activated mortars obtained from the alkali activation of fly ashes and containing a 20 wt% amount of waste glass as natural aggregate substitution have been formulated. Their rheological properties in the fresh state are improved when compared to the unmodified material. The microstructure of the mortars in terms of density and open porosity is almost unchanged as well as their mechanical properties.

Accelerated tests at 80 and 38°C underline an inert behaviour of the wastes towards expansive, deleterious reactions. Modified mortars show the same stability towards freeze-thaw cycles and sulphates diffusion as the unmodified ones. All the alkali activated composites are more stable that traditional Portland ones that are affected, at the same curing time, by Delayed Ettringite Formation (DEF) reaction and show the same stability towards freeze-thaw stresses.

From an environmental point of view, these results are quite interesting since lamp glass and the discarded fraction of glass urban collection cannot be reused in the production

of new glass items and cannot be recycled without previous chemical treatments in traditional binders containing Portland cement since they develop alkali-silica reactions. The absence of expansion reactions (either ASR or DEF) further promotes the use of alkali activated binders that are already considered as green, low carbon dioxide footprint materials.

References

[1] A. Majdinasab, Q. Yuan, Post-consumer cullet and potential engineering applications in North America, Res. Cons. Rec. 147 (2019) 1-9. https://doi.org/10.1016/j.resconrec.2019.04.009.

[2] European Waste Catalogue. Waste Framework Directive (2018) http://ec.europa.eu/environment/waste/framework/list.htm (accessed July 17, 2019).

[3] M. A. Imteaz, M.M.Y. Ali, A. Arulrajah, Possible environmental impacts of recycled glass used as a pavement base material, Waste Manag. Res. 30 (2012) 917-21. http://dx.doi.org/10.1177/0734242x12448512.

[4] A.R.G. de Azevedo, J. Alexandre, E.B. Zanelato, M.T. Marvila, Influence of incorporation of glass waste on the rheological properties of adhesive mortar, Constr. Build. Mater. 148 (2017) 359-368. https://doi.org/10.1016/j.conbuildmat.2017.04.208.

[5] A. Mohajerani, J. Vajna, T.H.H. Cheung, H. Kurmus, A. Arulrajah, S. Horpibulsuk, Practical recycling applications of crushed waste glass in construction materials: A review, Constr. Build. Mater. 156 (2017) 443-467.
https://doi.org/10.1016/j.conbuildmat.2017.09.005.

[6] C.C. Wang, H.Y. Wang, Assessment of the compressive strength of recycled waste LCD glass concrete using the ultrasonic pulse velocity, Constr. Build. Mater. 137 (2017) 345-353. https://doi.org/10.1016/j.conbuildmat.2017.01.117.

[7] K. Bisht, P.V. Ramana, Sustainable production of concrete containing discarded beverage glass as fine aggregate, Constr. Build. Mater. 177 (2018) 116-124. https://doi.org/10.1016/j.conbuildmat.2018.05.119.

[8] S.Y. Choi, Y.S. Choi, E.I. Yang, Characteristics of volume change and heavy metal leaching in mortar specimens recycled heavyweight waste glass as fine aggregate, Constr. Build. Mater. 165 (2018) 424-433.
https://doi.org/10.1016/j.conbuildmat.2018.01.050.

[9] A. Hajimohammadi, T. Ngo, A. Kashani, Sustainable one-part geopolymer foams with glass fines versus sand as aggregates, Constr. Build. Mater. 171 (2018) 223-231. https://doi.org/10.1016/j.conbuildmat.2018.03.120.

[10] I.S. Kim, S.Y. Choi, E.I. Yang, Evaluation of durability of concrete substituted heavyweight waste glass as fine aggregate, Constr. Build. Mater. 184 (2018) 269-277. https://doi.org/10.1016/j.conbuildmat.2018.06.221.

[11] J. X. Lu, C.S. Poon, Use of waste glass in alkali activated cement mortar, Constr. Build. Mater. 160 (2018) 399-407. https://doi.org/10.1016/j.conbuildmat.2017.11.080.

[12] N. Arabi, H. Meftah, H. Amara, O. Kebaïli, L. Berredjem, Valorization of recycled materials in development of self-compacting concrete: Mixing recycled concrete aggregates – Windshield waste glass aggregates, Constr. Build. Mater. 209 (2019) 364-376. https://doi.org/10.1016/j.conbuildmat.2019.03.024.

[13] A. Hajimohammadi, T. Ngo, J. Vongsvivut, J. Interfacial chemistry of a fly ash geopolymer and aggregates, J. Clean. Prod. 231 (2019) 980-989. https://doi.org/10.1016/j.jclepro.2019.05.249.

[14] Y. Liu, C. Shi, Z. Zhang, N. Li, An overview on the reuse of waste glasses in alkali-activated materials, Res. Cons. Rec. 144 (2019) 297-309. https://doi.org/10.1016/j.resconrec.2019.02.007.

[15] J. X. Lu, H. Zheng, S. Yang, P- He, C.S. Poon, Co-utilization of waste glass cullet and glass powder in precast concrete products, Constr. Build. Mater. 223 (2019) 210-220. https://doi.org/10.1016/j.conbuildmat.2019.06.231.

[16] S. Luhar, I. Luhar, Potential application of E-wastes in construction industry: A review, Constr. Build. Mater. 203 (2019) 222-240. https://doi.org/10.1016/j.conbuildmat.2019.01.080.

[17] A. Mohammadinia, Y.C. Wong, A. Arulrajah, S. Horpibulsuk, Strength evaluation of utilizing recycled plastic waste and recycled crushed glass in concrete footpaths, Constr. Build. Mater. 197 (2019) 489-496.
https://doi.org/10.1016/j.conbuildmat.2018.11.192.

[18] S.B. Park, B.C. Lee, J. Kim, Studies on the mechanical properties of concrete containing waste glass aggregate. Cem. Concr. Res. 34 (2004) 2181-2189.
https://doi.org/10.1016/j.cemconres.2004.02.006.

[19] V. Corinaldesi, G. Gnappi, G. Moriconi, A. Montenero, Reuse of ground waste glass as aggregate for mortars, Waste Manag. 25 (2005) 197–201.
https://doi.org/10.1016/j.wasman.2004.12.009.

[20] M. Limbachija, Bulk engineering and durability properties of washed glass sand concrete, Constr. Build. Mater. 23 (2009) 1078-83.
https://doi.org/10.1016/j.conbuildmat.2008.05.022.

[21] S. De Castro, J. De Brito, Evaluation of the durability of concrete made with crushed glass aggregates, J. Clean. Prod. 41 (2013) 7-14.
https://doi.org/10.1016/j.jclepro.2012.09.021.

[22] K.H. Tan, H. Du, Use of waste glass as sand in mortar: Part I – Fresh, mechanical and durability properties, Cem. Concr. Res. 35 (2013) 109-117.
https://doi.org/10.1016/j.cemconcomp.2012.08.028.

[23] A. Rashad, Recycled waste glass as fine aggregate replacement in cementitious materials based on Portland cement, Constr. Build. Mater. 72 (2014) 340-357. https://doi.org/10.1016/j.conbuildmat.2014.08.092.

[24] M. Mavroulidou, S. Awoliyi, A study on the potential use of paper sludge ash in concrete with glass aggregate, Waste Manag. Res. 36 (2018) 1061-65. https://doi.org/10.1177/0734242X18801196.

[25] H. Wang, A study of the effects of LCD glass on the properties of concrete, Waste Manag. 29 (2009) 335-341. https://doi.org/10.1016/j.wasman.2008.03.005.

[26] D. Romero, J. James, R. Mora, Study on the mechanical and environmental properties of concrete containing CRT glass aggregate, Waste Manag. 33 (2013) 1659-666. https://doi.org/10.1016/j.wasman.2013.03.018.

[27] A. Rashad, Recycled cathode ray tube and liquid crystal display glass as fine aggregate replacement in cementitious materials, Constr. Build. Mater. 93 (2015) 1236-1248. https://doi.org/10.1016/j.conbuildmat.2015.05.004.

[28] A. Saccani, M.C. Bignozzi, L. Barbieri, I. Lancellotti, E. Bursi, Effect of the chemical composition of different types of recycled glass used as aggregates on the ASR performance of cement mortars, Constr. Build. Mater. 154 (2017) 804–809. https://doi.org/10.1016/j.conbuildmat.2017.08.011.

[29] S.Y. Choi, Y.S. Choi, E.I. Yang, Characteristics of volume change and heavy metal leaching in mortar specimens recycled heavyweight waste glass as fine aggregate, Constr. Build. Mater. 165 (2018) 424-433. https://doi.org/10.1016/j.conbuildmat.2018.01.050.

[30] A. Saccani, F. Sandrolini, F. Andreola, L. Barbieri, A. Corradi, I. Lancellotti, Influence of the pozzolanic fraction obtained from vitrified bottom ashes from MSWI on the properties of cementitiuos composites, *Mater. Struct. 38* (2005) 367-71. DOI: 10.1617/14173.

[31] M. Bignozzi, A. Saccani, F. Sandolini, Matt waste from glass separated collection: an eco-sustainable addition for new building materials, Waste Manag. 29 (2009) 329-334. doi:10.1016/j.wasman.2008.02.028

[32] Y. Kawabata, K. Yamada, Evaluation of alkalinity of pore solution based on the phase composition of cement hydrates with supplementary cementitious materials and its relation to suppressing ASR expansion, J. Advanced Concr. Technol. 13 (2015) 538-553. https://doi.org/10.3151/jact.13.538.

[33] S.M.H. Shafaatian, J.R. Wright, F. Rajabipour, Performance of recycled soda-lime glass powder in mitigating alkali-silica reaction, Green Mater. 7 (2019) 28-39. https://doi.org/10.1680/jgrma.18.00032.

[34] T. Okada, F. Nishimura, S. Yonezawa, Removal of lead from cathode ray tube funnel glass by combined thermal treatment and leaching process, Waste Manag. 45 (2015) 343-350. https://doi.org/10.1016/j.jhazmat.2015.11.032.

[35] X. Mingfei, W. Yaping, L. Jun, X. Hua, Lead recovery and glass microspheres synthesis from waste CRT funnel glasses through carbon thermal reduction enhanced acid leaching process, J. Hazard. Mater. 305 (2016) 51–58.
https://doi.org/10.1016/j.jhazmat.2015.11.032.

[36] E. Bursi, L. Barbieri, I. Lancellotti, A. Saccani, M. Bignozzi, Lead waste glasses management: Chemical pretreatment for use in cementitious composites, Waste Manag. Res. 35 (2017) 958-966. https://doi.org/10.1177/0734242X17715098.

[37] M.C. Bignozzi, S. Manzi, I. Lancellotti, E. Kamseu, L. Barbieri, C. Leonelli, Mix-design and characterization of alkali activated materials based on metakaolin and ladle slag, Appl. Clay Sci. 73 (2013) 78-85. http://dx.doi.org/10.1016/j.clay.2012.09.015.

[38] J.L. Provis, A. Palomo, C. Shi, Advances in understanding alkali-activated materials, Cem. Concr. Res. 78 (2015), 110-125.
https://doi.org/10.1016/j.cemconres.2015.04.013.

[39] L. Carabba, M. Santandrea, C. Carloni, S. Manzi, M.C. Bignozzi, Steel fiber reinforced geopolymer matrix (S-FRGM) composites applied to reinforced concrete structures for strengthening applications: A preliminary study, Composites. Part B, Eng. 128 (2017) 83-90. https://doi.org/10.1016/j.compositesb.2017.07.007.

[40] J.L. Provis, Alkali-activated materials, Cem. Concr. Res. 114 (2018) 40-48. https://doi.org/10.1016/j.cemconres.2017.02.009.

[41] K. Kupwade-Patil, E. Allouche, Impact of alkali silica reaction on fly ash-based geopolymer concrete, J. Mater. Civ. Eng. 25 (2013) 131-139. https://doi.org/10.1061/(ASCE)MT.1943-5533.0000579.

[42] R. Pouhet, M. Cyr, Alkali–silica reaction in metakaolin-based geopolymer mortar, Mater. Struct. 48 (2015) 571–583. DOI 10.1617/s11527-014-0445-x.

[43] Y. Liu, C. Shi, Z. Zhang, N. Li, An overview on the reuse of waste glasses in alkali-activated materials, Res. Cons. Rec. 144 (2019) 297–309. https://doi.org/10.1016/j.resconrec.2019.02.007.

[44] E. Bursi, I. Lancellotti, L. Barbieri, A. Saccani, M. Bignozzi, Chelating agent treatment on leaded residuals from glass separated urban collection to be used in cement mortars, Waste Bio. Valor. 9 (2018) 2493-2501. https://doi.org/10.1007/s12649-018-0254-5.

[45] A. Pereira, J.L. Akasaki, J.L.P. Melges, M.M. Tashima, L. Soriano, M.V. Borrachero, J. Monzó, J. Payá, Mechanical and durability properties of alkali-activated mortar based on sugarcane bagasse ash and blast furnace slag, Ceram. Int. 41 (2015) 13012–13024. https://doi.org/10.1016/j.ceramint.2015.07.001.

[46] F. Slaty, H. Khourya, H. Rahier, J. Wastiels, Durability of alkali activated cement produced from kaolinitic clay, Appl. Clay Sci. 104 (2015) 229–237.

https://doi.org/10.1016/j.clay.2014.11.037.

[47] K. Arbi, M. Nedeljkovic, Y. Zuo, G. Ye, A review on the durability of alkali-activated fly ash/slag systems: advances, issues and perspectives, Industrial Eng. Chem. Res. 55 (2016) 5439-5453. https://doi.org/10.1021/acs.iecr.6b00559.

[48] M. Zhang, M. Zhao, D. Zhang, D. Mann, K. Lumsden, M. Tao, Durability of red mud-fly ash based geopolymer and leaching behavior of heavy metals in sulfuric acid solutions and deionized water, Constr. Build. Mater. 124 (2016) 373–382. https://doi.org/10.1016/j.conbuildmat.2016.07.108.

[49] H. Rashidian-Dezfouli, P.R. Rangaraju, A comparative study on the durability of geopolymers produced with ground glass fiber, fly ash, and glass-powder in sodium sulfate solution, Constr. Build. Mater. 153 (2017) 996-1009.

https://doi.org/10.1016/j.conbuildmat.2017.07.139.

[50] EN 196-1: Methods of testing cement – Part 1: determination of strength (2016).

[51] EN 1015-3: Determination of consistence of fresh mortars by flow table (2007).

[52] EN 772-13: Determination of net and gross dry density (2002).

[53] EN 772-21: Determination of water absorption (2011).

[54] ASTM C1260: Standard test method for potential alkali reactivity of aggregates (Mortar-Bar Method) (2014).

[55] ASTM C666: Standard test method for resistance of concrete to rapid freezing and thawing (2015).

[56] L. Jian-Ling, C.H. Poon, Use of waste glass in alkali activated cement mortar, Constr. Build. Mater. 160 (2018) 399-407. https://doi.org/10.1016/j.conbuildmat.2017.11.080.

[57] A. Hajimohammadi, T. Ngo, A. Kashani, Glass waste versus sand as aggregates: the characteristics of the evolving geopolymer binders, J. Clean. Prod. 193 (2018) 593-603. https://doi.org/10.1016/j.jclepro.2018.05.086.

Table 1. Oxide content of the investigated materials.

Material	SiO_2	Al_2O_3	Na_2O	K_2O	CaO	MgO	PbO	BaO	Fe_2O_3	SO_3	LOI
RUB	66.25	1.88	9.42	5.98	5.60	1.65	6.91	2.21	0.00	0.00	0.00
LMP	68.47	2.26	17.65	1.61	5.13	2.98	0.79	0.95	0.00	0.00	0.00
Fly ash	49.37	29.23	0.05	0.60	6.63	1.05	0.00	0.00	2.71	0.33	3.28

Table 2. Composition and labelling of all investigated samples.

Mortar sample	Natural sand (g)	Glass waste (g)	Sodium silicate solution (g)	NaOH 8M solution (g)	H_2O (g)	Fly ash (g)	Portland cement (g)
M-REF	1350	0	188	38	35	500	-
M-RUB	1080	270	188	38	35	500	-
M-LMP	1080	270	188	38	35	500	-
M-PRT	1350	0	0	0	225	-	450

Table 3. Physical properties of the investigated mortars.

Sample	M-REF	M-LMP	M-RUB	M-PRT
Workability (%)	59.1 ± 0.6	69.6 ± 0.9	69.0 ± 0.4	41.3 ± 0.8
Density (g/cm^3)	2.11	2.07	2.03	2.11
Porosity (vol %)	10.76	10.69	10.86	19.50

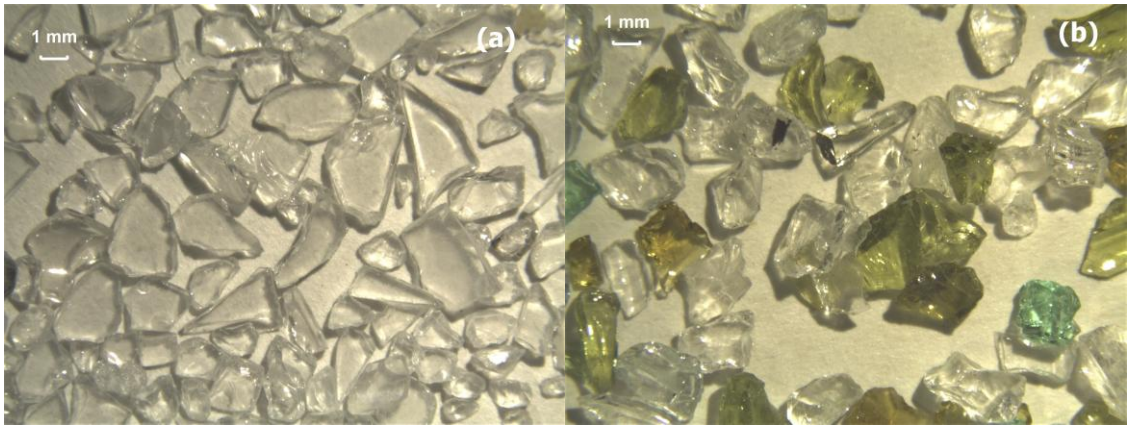

Fig. 1. Morphology of LMP (a) and RUB (b) cullets.

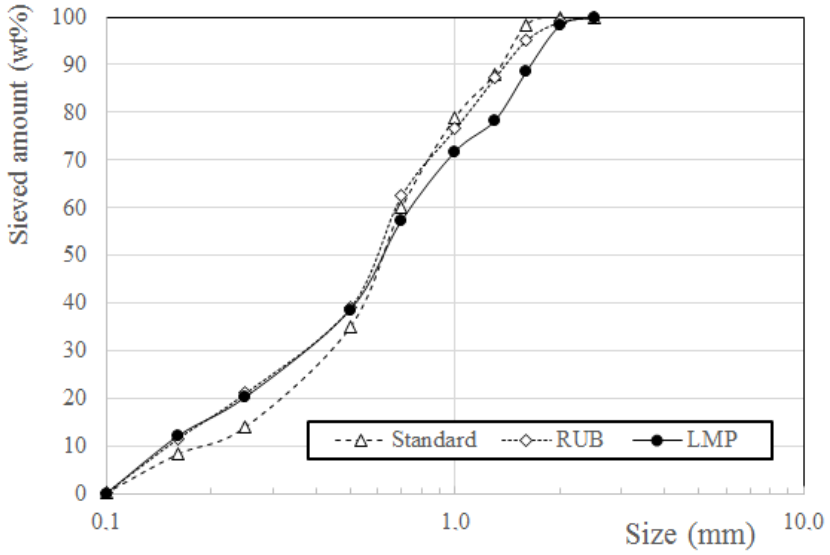

Fig. 2. Size distribution of natural sand and glass cullets.

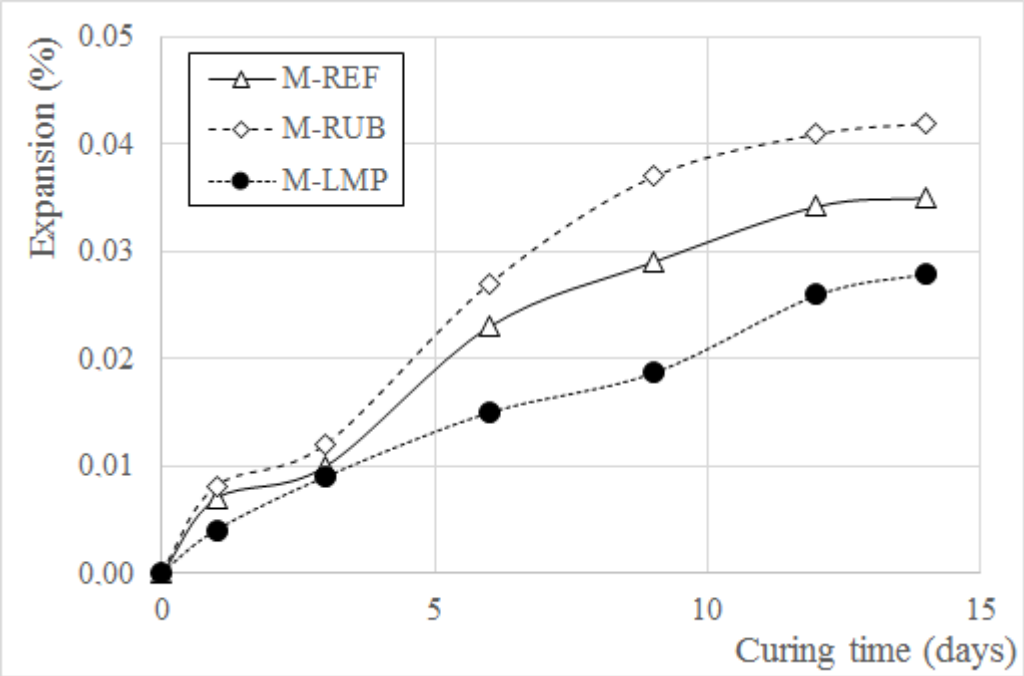

Fig. 3. Expansion at 80°C.

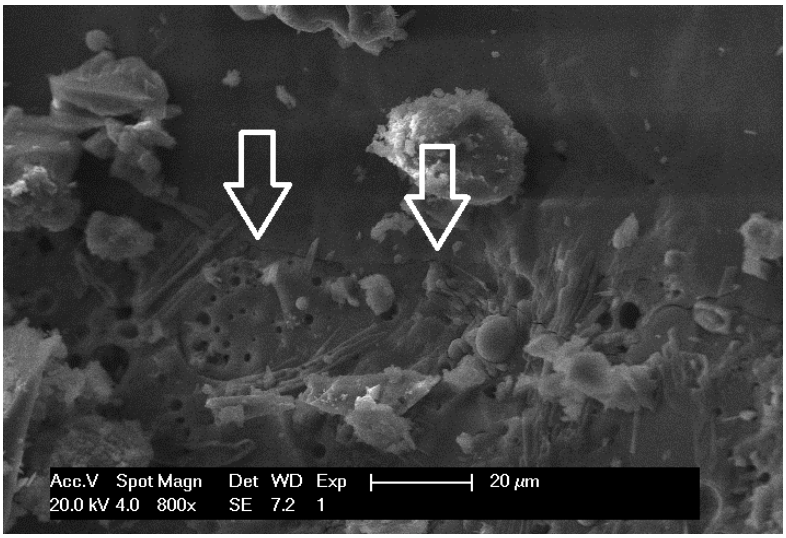

Fig. 4. Sharp unreacted contour (arrows) of one LMP cullet in contact with the alkali activated matrix (fracture surface of M-LMP cured at 80°C in NaOH solution).

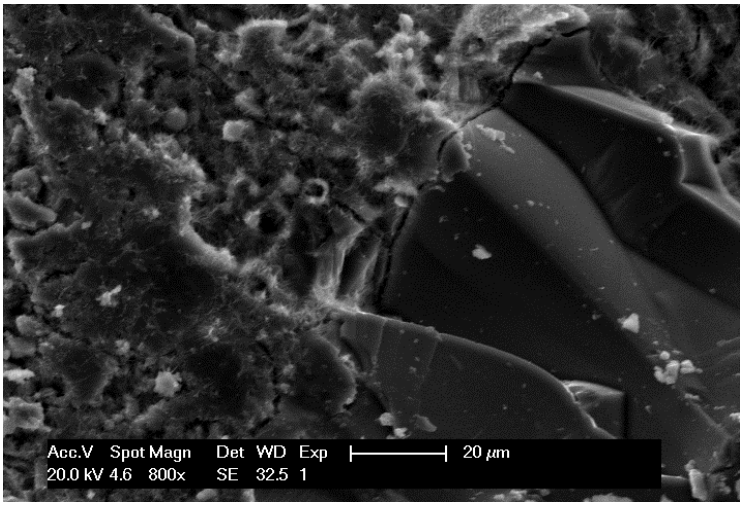

Fig. 5. Sharp unreacted RUB cullet cured at 80 °C in NaOH solution from M-RUB mortar.

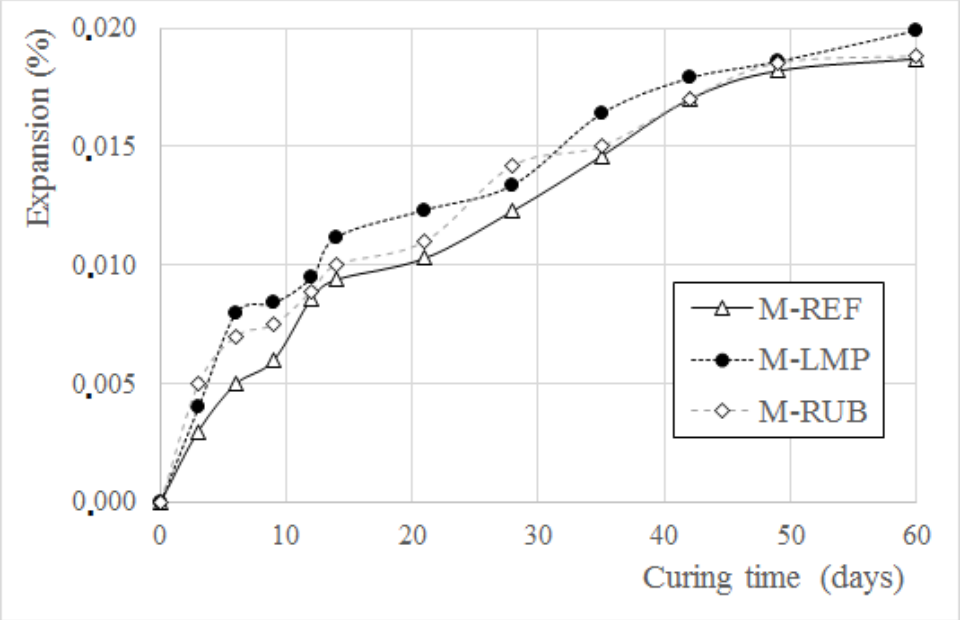

Fig. 6. Expansion vs curing time at 38°C.

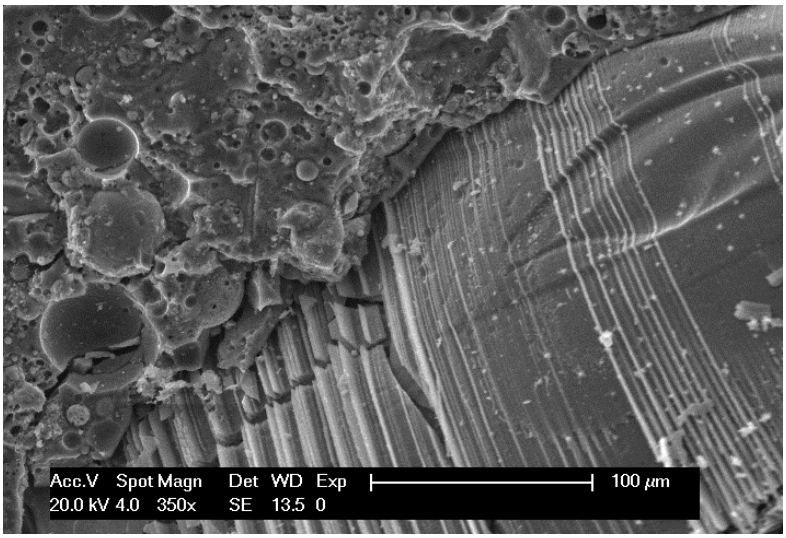

Fig.7. Unreacted LMP cullet at 60 days of curing (38 °C) for M-LMP mortar.

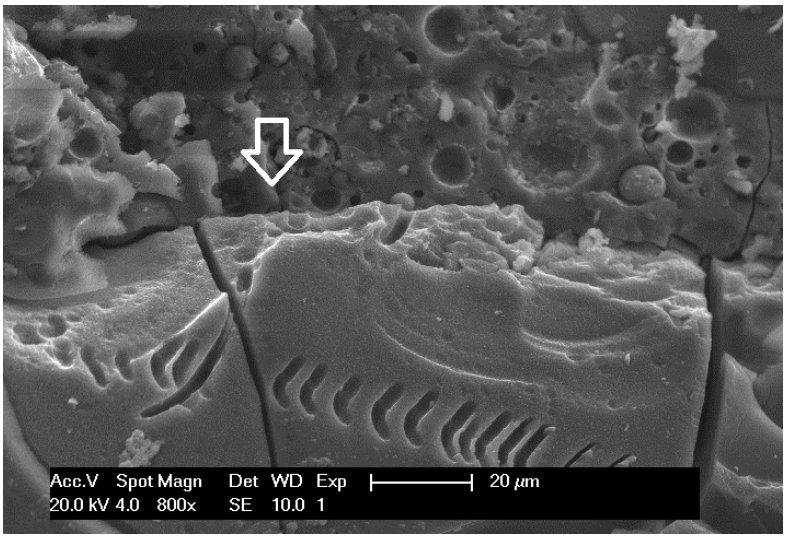

Fig. 8. Unreacted RUB cullet at 60 days of curing (38°C) for M-RUB mortar.

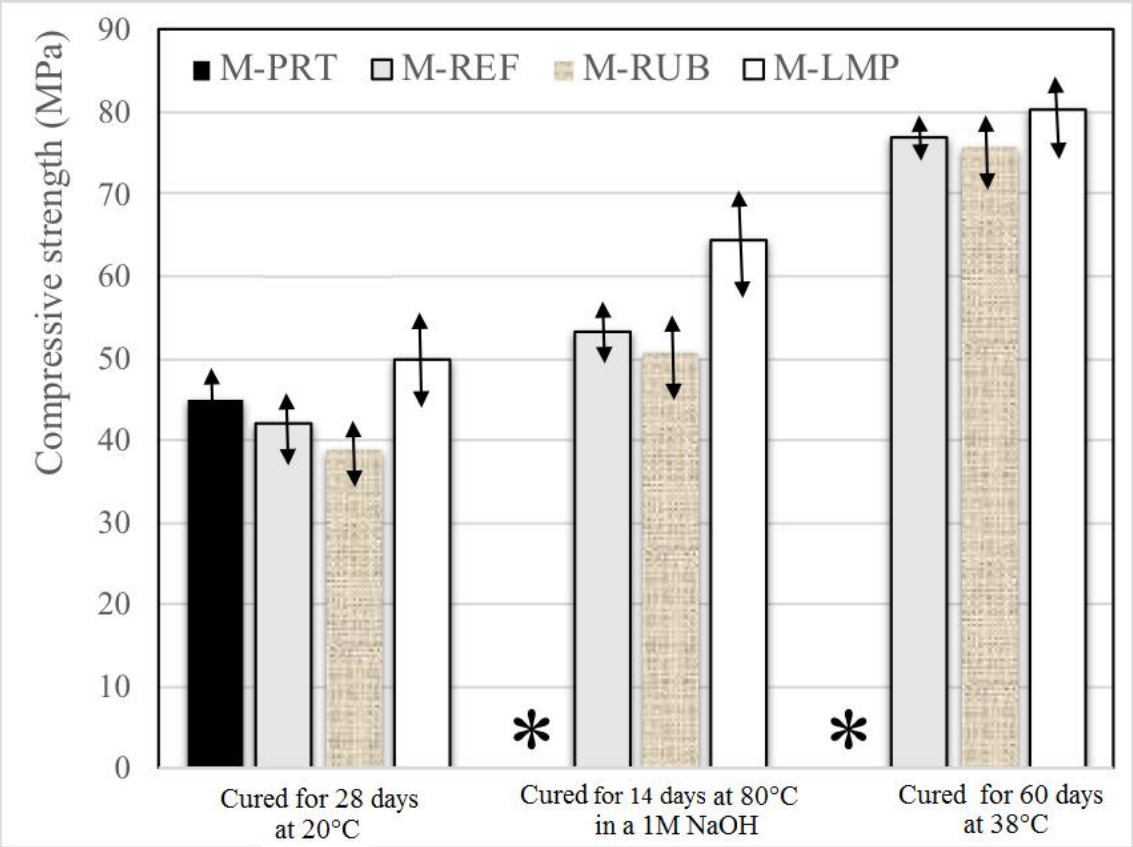

Fig. 9. Mechanical properties of samples in different curing conditions.

(*) Portland samples not reported since showing expanding behaviour

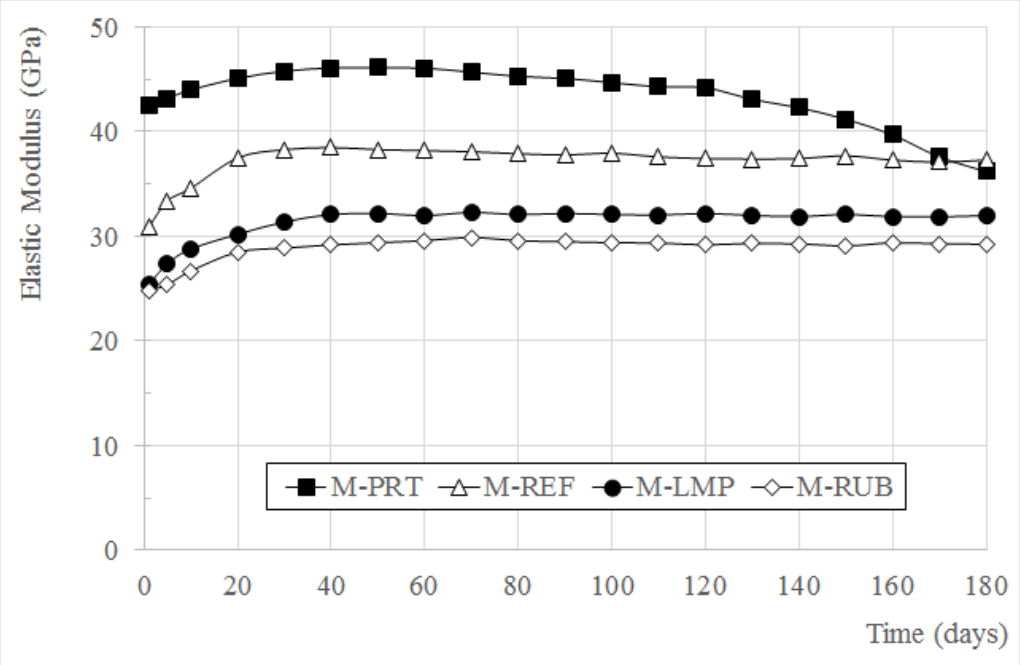

Fig. 10. Plot of the dynamic elastic modulus vs time of mortars in sulphates solution.

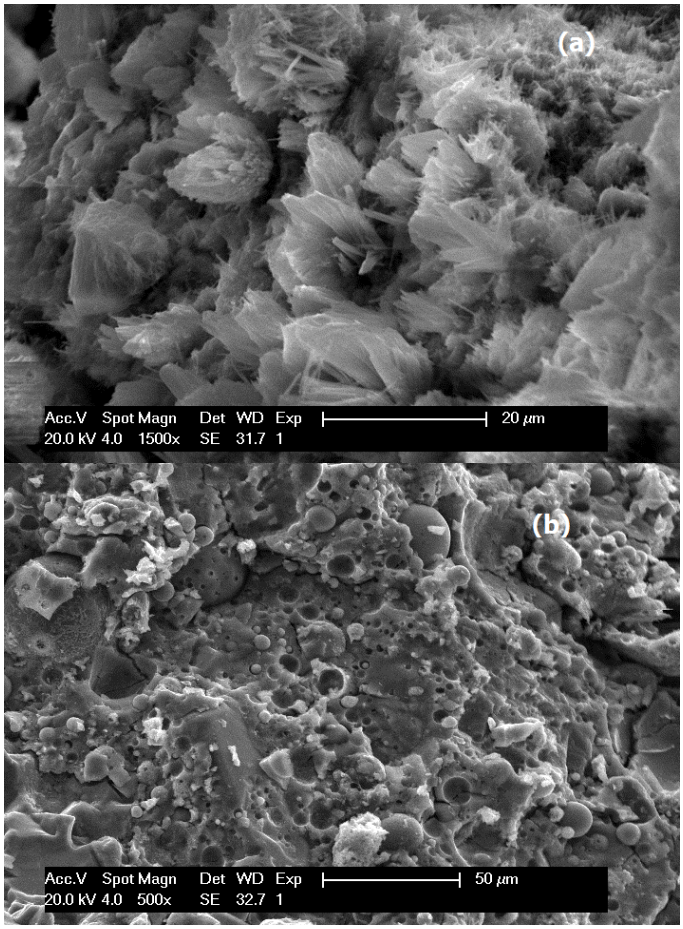

Fig. 11. (a) ettringite samples in M-PRT sample (b) alkali activated matrix of M-RUB sample.

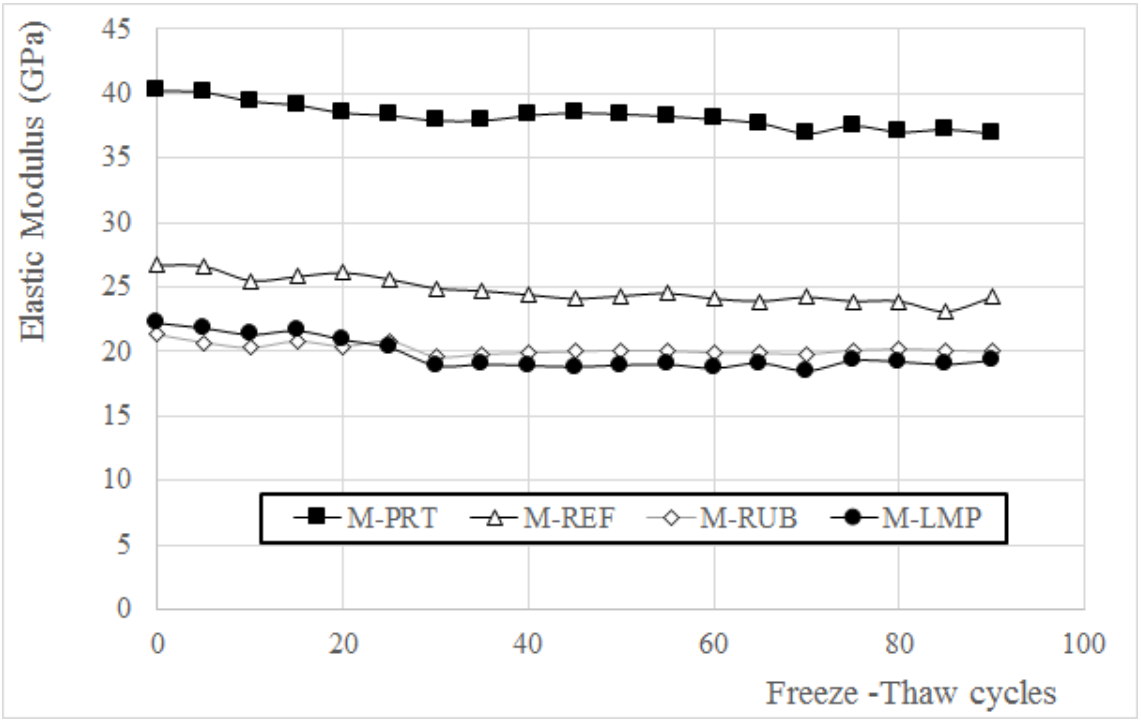

Fig. 12. Elastic modulus vs freeze-thaw cycles.